Resistivity studies under hydrostatic pressure on a low-resistance variant of the quasi-two-dimensional organic superconductor κ-(BEDT-TTF)$_2$Cu[N(CN)$_2$]Br: Search for intrinsic scattering contributions

Ch. Strack, C. Akinci, V. Pashchenko, B. Wolf, E. Uhrig, W. Assmus, and M. Lang
Physikalisches Institut, J.W. Goethe-Universität Frankfurt(M), FOR 412, D-60054 Frankfurt am Main, Germany

J. Schreuer and L. Wiehl
Institut für Mineralogie, J.W. Goethe-Universität Frankfurt(M), FOR 412, D-60054 Frankfurt am Main, Germany

J. A. Schlueter
Materials Science Division, Argonne National Laboratory, Argonne, Illinois 60439, USA

J. Wosnitza*
Institut für Festkörperphysik, TU Dresden, 01062 Dresden, Germany

D. Schweitzer
3. Physikalisches Institut, Universität Stuttgart, D-70550 Stuttgart, Germany

J. Müller
Center for Materials Research and Technology, Florida State University, Tallahassee, Florida 32306-4351, USA

J. Wykhoff
Max Planck Institut für Chemische Physik fester Stoffe, D-01187 Dresden, Germany
(Received 13 July 2004; revised manuscript received 24 May 2005; published 10 August 2005)

Resistivity measurements have been performed on a low (LR)- and high (HR)-resistance variant of the κ-(BEDT-TTF)$_2$Cu[N(CN)$_2$]Br superconductor. While the HR sample was synthesized following the standard procedure, the LR crystal is a result of a somewhat modified synthesis route. Judging by their residual resistivities and residual resistivity ratios, the LR crystal is of distinctly superior quality. He-gas pressure was used to study the effect of hydrostatic pressure on the different transport regimes for both variants. The main results of these comparative investigations are (i) a significant part of the inelastic-scattering contribution, which causes the anomalous $\rho(T)$ maximum in standard HR crystals around 90 K, is sample dependent, i.e., extrinsic in nature; (ii) the abrupt change in $\rho(T)$ at $T^* \approx 40$ K from a strongly temperature-dependent behavior at $T > T^*$ to an only weakly T-dependent $\rho(T)$ at $T < T^*$ is unaffected by this scattering contribution and thus marks an independent property, most likely a second-order phase transition, and (iii) both variants reveal a $\rho(T) \propto AT^2$ dependence at low temperatures, i.e., for $T_c \leqslant T \leqslant T_0$, although with strongly sample-dependent coefficients A and upper bounds for the T^2 behavior measured by T_0. Provided that there are no differences in the Fermi surface between both variants—the present experiments give no indications for such differences—the latter result is inconsistent with the T^2 dependence originating from coherent Fermi-liquid excitations.

DOI: 10.1103/PhysRevB.72.054511 PACS number(s): 72.15.Eb, 72.80.Le, 74.70.Kn

I. INTRODUCTION

Organic charge-transfer salts, based on the electron-donor molecule BEDT-TTF (bis-ethylenedithiotetrathiafulvalene)—or simply ET—form layered structures consisting of alternating sheets of conducting $(ET)_2^+$ cations and insulating anions X^-. Within this class of materials, the κ-phase $(ET)_2X$ salts with X=Cu[N(CN)$_2$]Cl, Cu[N(CN)$_2$]Br, and Cu(NCS)$_2$ are of particular interest due to the variety of electronic phases encountered as a function of hydrostatic pressure or anion substitution. According to the conceptual phase diagram proposed by Kanoda, the ground state of the system is controlled by the parameter W/U_{eff}, i.e., the width of the conduction band W relative to the effective on-site Coulomb repulsion U_{eff}, a ratio which can be changed by hydrostatic pressure or chemical substitutions.[1] This conceptual phase diagram implies that the antiferromagnetic insulator X=Cu[N(CN)$_2$]Cl and the correlated metal X=Cu[N(CN)$_2$]Br lie on opposite sites of a bandwidth-controlled Mott transition. The region across this metal-to-insulator transition has been explored in great detail by employing pressure studies of various magnetic,[2] transport,[3,4] and acoustic[5] properties. These studies confirm earlier results[6,7] which revealed that at a pressure of 300–400 bar, i.e., above the critical region of coexistence of insulating and metallic phases,[2,4] the X=Cu[N(CN)$_2$]Cl salt shows the same highly unusual resistivity profile $\rho(T)$ as the Cu[N(CN)$_2$]Br system at ambient pressure. Three distinct transport regimes have been identified:[4] (*i*) a *semiconducting* high-temperature range, (*ii*) a *bad metal* behavior at intermediate temperatures

with a strongly temperature-dependent $\rho(T)$ and a pronounced maximum around 90 K that marks the crossover to regime (*i*), and (*iii*) a $\rho \propto AT^2$ behavior at low temperatures preceding the superconducting transition at T_c. Various explanations have been proposed for the different transport regimes. Suggestions for the anomalous resistance maximum include an order-disorder transition of the ethylene endgroups of the ET molecules[8–10] and a crossover from localized small-polaron to coherent large polaron behavior[11] (see also Ref. 12 for earlier arguments on the resistance anomaly). Alternatively, the "*bad metal*" regime (*ii*) together with the T^2 dependence at low temperatures have been linked to the strongly correlated nature of the electrons.[4,13] Within a dynamical mean-field (DMFT) approach, Merino *et al.*[13] predicted a smooth crossover from coherent Fermi liquid excitations with $\rho \propto T^2$ at low temperatures to incoherent (*bad metal*) excitations at higher temperatures. Using such DMFT calculations for a simple Hubbard model, Limelette *et al.*[4] recently attempted to provide even a quantitative account for the $\rho(T)$ behavior of pressurized $X=Cu[N(CN)_2]Cl$ over an extended temperature range covering almost all three of the above-cited transport regimes (i)–(iii). On the other hand, it has been found by transport studies on the present $X=Cu[N(CN)_2]Br$ system,[14] the alloy $X=Cu[N(CN)_2]Cl_{1-x}Br_x$ (Ref. 15) as well as the related $X=Cu[N(CN)_2]I$ salt (see Ref. 16 and references cited therein) that the resistivity profiles may change significantly depending on the conditions under which the materials have been synthesized.

It is thus fair to say that, despite the intensive efforts from both experimental and theoretical sides to explain the anomalous state above T_c, its nature still remains puzzling. In that respect, a deeper understanding of the unusual $\rho(T)$ behavior would be of paramount importance given that the inelastic-scattering mechanism, which causes the electrical resistivity of a superconductor above T_c, is usually identical to the relevant pairing interaction.

In this paper, we report resistivity measurements on different variants of the $X=Cu[N(CN)_2]Br$ superconductor which have been prepared along different routes: a high-resistance (HR) variant prepared according to the standard procedure and three crystals, #2, #3, and a low-resistance (LR) sample, synthesized under somewhat modified preparation conditions. These comparative studies, which include measurements under hydrostatic pressure, disclose strikingly sample-dependent transport properties. Our results demonstrate that, in contrast to conventional metals obeying Matthiessen's rule, extrinsic factors such as disorder or defects may strongly affect the inelastic scattering contribution in the present molecular conductors.

II. EXPERIMENTAL

The single crystals of κ-(BEDT-TTF)$_2$Cu[N(CN)$_2$]Br were prepared using two different preparation routes. The HR single crystal was synthesized at Argonne National Laboratory following the standard procedure as described elsewhere.[17] The crystals #2, #3, and the LR crystal were grown at the University of Stuttgart by solving 60 mg BEDT-TTF, 80 mg tetraphenylphosphoniumdicyanamid [$Ph_4PN(CN)_2$], and 20 mg CuBr in a mixture of 80 ml tetrahydrofuran (THF) and 20 ml ethylenglycol (EG). For the starting materials the highest possible grades were used. The solution was filled in a three-chamber electrochemical cell. The crystals were then grown at a current of 35 μA and a voltage of 1.3 V applied over a period of 14 days.

TABLE I. Unit cell parameters of the HR crystal and #3 of κ-(BEDT-TTF)$_2$Cu[N(CN)$_2$]Br taken at 295 K and at 100 K together with literature results.

	#3 295 K	#3 100 K	HR 295 K	HR 100 K	Ref. 17 298 K
a(Å)	12.955(2)	12.895(2)	12.957(2)	12.905(2)	12.942(3)
b(Å)	29.998(3)	29.630(3)	29.993(3)	29.614(3)	30.016(4)
c(Å)	8.545(1)	8.483(1)	8.547(1)	8.478(1)	8.539(3)
V(Å^3)	3321(1)	3241(1)	3322(1)	3240(1)	3317(1)

The crystals have been first characterized by electron probe microanalysis (EPMA) using an energy dispersive x-ray detector (EDAX PV 9802) adopted to a 30 keV scanning electron microscope. As a partial substitution of bromine by chlorine is known to result in drastic changes in the resistivity profile,[15,18,19] particular care was taken to track possible chlorine contaminations. Within the resolution of our EPMA measurements of 1–2 at %, all samples reveal identical spectra with the same relative peak intensities and were found to be free of any chlorine contribution.

Further, single-crystal structure determinations were performed on the samples #3 and the HR crystal, i.e., one sample from each preparation route. Data have been collected at 295 K and 100 K using an Xcalibur four-circle diffractometer from Oxford Diffraction with a $2k \times 2k$ CCD detector (Sapphire3) and Mo $K\alpha$ radiation ($\lambda = 0.710\,73$ Å). For the low-temperature measurements, the crystals were cooled with a nitrogen gas stream supplied by an Oxford cryojet. On each sample, more than 60 000 (partly redundant) reflections were collected within a full sphere up to an angle of $2\theta = 48°$. The lattice parameters were refined from the diffraction angles of the complete data sets. After empirical absorption correction, the intensity data were merged to about 2600 unique reflections. Systematic absences of reflections at both temperatures correspond to space group *Pnma*. The structures were solved by direct methods [SHELXS-97 (Ref. 20)] and the atom coordinates and the anisotropic displacement parameters for nonhydrogen atoms were refined against F^2 [SHELXL-97 (Ref. 20)] leading to final figures of merit ($R1$, $wR2$) of 0.051, 0.087 (HR at 295 K); 0.046, 0.081 (HR at 100 K); 0.053, 0.089 (#3 at 295 K), and 0.050, 0.104 (#3 at 100 K), respectively.

The lattice parameters at 295 K and 100 K are listed in Table I together with the room-temperature data reported by Kini *et al.*[17] on a crystal prepared according to the standard procedure. Within the absolute accuracy, the lattice parameters and the unit cell volumes at 295 K for the two crystals studied here and the numbers given by Kini *et al.*[17] agree well.

In addition, comparative ESR measurements have been carried out on fragments of two crystals, the HR and #3, after

completion of the resistivity measurements. Data have been taken at five different temperatures between 300 K and 15 K using a Bruker ELEXYS E500 X-band spectrometer. A geometry was chosen with the static magnetic field aligned perpendicular to the conducting (a,c) plane and with the sample rotating around an in-plane axis. At room temperature, both crystals reveal an approximate Lorentzian line with the same peak-to-peak width of $\Delta H_{pp}=(60\pm1)$ G for $B\|b$ consistent with literature results[21–23] on materials prepared according to the standard procedure. Upon cooling, the line was found to broaden slightly for both crystals in the same way yielding $\Delta H_{pp}=(72\pm1)$ G [150 K], (79 ± 1) G [100 K], and (85 ± 2) G [50 K]. In addition, the spectra of both crystals contained a narrow line of width $\Delta H_{pp}=(13\pm0.5)$ G located at about the same resonance field as the above broad line of (3351 ± 0.5) G. The relative intensity of the narrow line, which was smaller for crystal #3 and which lacked any angular dependence, was found to follow roughly a Curie-like increase upon cooling. A similar sample-dependent narrow line, besides the main signal, was also found in some crystals studied in Ref. 22, where it has been attributed to the presence of paramagnetic centers caused by crystal defects such as stable radicals. For the present materials, these defects may originate from the imperfect surface conditions of the crystal fragments after completion of the resistivity measurements. Attempts to determine accurately the linewidth at 15 K proved unsuccessful because of the presence of this additional narrow line which predominates the spectra at low temperatures.

The temperature dependence of the resistivity was measured employing a standard four-terminal ac technique operating at a frequency of 17 Hz. A maximum current of 10 μA was used to avoid self-heating. The electrical contacts to the crystal were made by 25 μm Cu wires attached to the sample by graphite paste. Typical contact resistances were $\leqslant 10\ \Omega$. Owing to the large in-plane vs. out-of-plane resistivity anisotropy in these materials and the irregular shape of the crystals, an accurate determination of the in-plane resistivity $\rho_\|$ is very difficult, see, e.g., Refs. 24–26. As pointed out in these references, those in-plane data derived from a standard measurement geometry with four contacts on the same face of the crystal almost always contain a significant interlayer component $\rho_\perp$. Thus, most reliable resistivity data, free of such mixing effects, can be obtained from out-of-plane measurements. To rule out errors which might originate in an inhomogeneous current flow in our four-terminal out-of-plane measurements, comparative investigations using a six-terminal configuration were conducted and found to deviate by not more than 4% at maximum. For the latter measurement geometry, the current had been fed through the crystal by two pairs of terminals (the outer two of three terminals) attached to opposite crystal surfaces assuring these surfaces to be equi-potential planes. These $\rho_\perp$ data enable even a quantitative comparison with corresponding results on other crystals to be performed. For the in-plane measurements, $\rho_\|$, the current contacts were placed on opposite end surfaces of the crystal. A He-gas-pressure technique was used to ensure hydrostatic pressure conditions. The measurements were performed at a low sweep rate of 0.1 K min^{-1} to guarantee thermal equilibrium and to minimize effects associated with disorder in the ethylene groups which may arise from rapidly cooling through the glass transition at $T_g=77$ K.

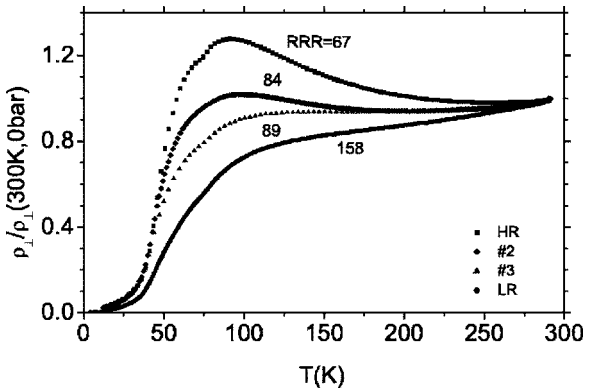

FIG. 1. Temperature dependence of the normalized interlayer resistivity of various single crystalline samples of κ-(BEDT-TTF)$_2$Cu[N(CN)$_2$]Br. RRR denotes the residual resistivity ratio as defined in the text.

III. RESULTS

Figure 1 gives an overview of the interlayer resistivities at ambient pressure for all four samples investigated. The data have been normalized to the room-temperature resistivity values in units of Ω cm of (35.5 ± 7))(HR), (45.3 ± 9) (#2), (40.7 ± 8) (#3), and (50.5 ± 12) (LR), where the error bars account for the uncertainties in determining the geometric factors. The figure also contains the values for the residual resistivity ratio RRR$=\rho_\perp(300\ \mathrm{K})/\rho_{0\perp}$ for the various crystals, with the residual resistivity ρ_0 determined by extrapolating the normal-state resistivity to $T=0$. As Fig. 1 clearly demonstrates, the resistivity profiles are strongly sample dependent: while $\rho_\perp(T)$ for the HR crystal shows the well-known behavior with a semiconducting increase at higher temperatures followed by the pronounced maximum around 90 K, the resistivity curves for the other crystals reveal a much weaker variation with temperature. In particular $\rho_\perp(T)$ for #3 and the LR crystal remains metallic below 300 K with a shoulder-like anomaly near 100 K. The latter feature is likely to be a remnant of the 90 K maximum that predominates the resistivity for the HR crystal.

In Fig. 2 we show the resistivity profiles $\rho(T)$ for the LR [Figs. 2(a) and 2(b)] and HR [Fig. 2(c)] single crystals at various pressures up to 2000 bar. Interestingly enough, while the out-of-plane resistivity for the LR crystal stays metallic below 300 K, a semiconducting-like increase with a maximum around 100 K is found for the in-plane resistivity [Fig. 2(b)]. For the resistivity anisotropy, $\rho_\perp/\rho_\|$, our measurements reveal a lower limit of about 100 at room temperature.

Apart from these sample-dependent contributions, the $\rho(T)$ data for both crystals exhibit a sharp dip at $T_g=77$ K. This anomaly has been assigned to a glass transition associated with a freezing of orientational degrees of freedom of the ethylene endgroups.[27,28]

With increasing pressure, the out-of-plane resistivity for both crystals becomes substantially reduced. This effect is

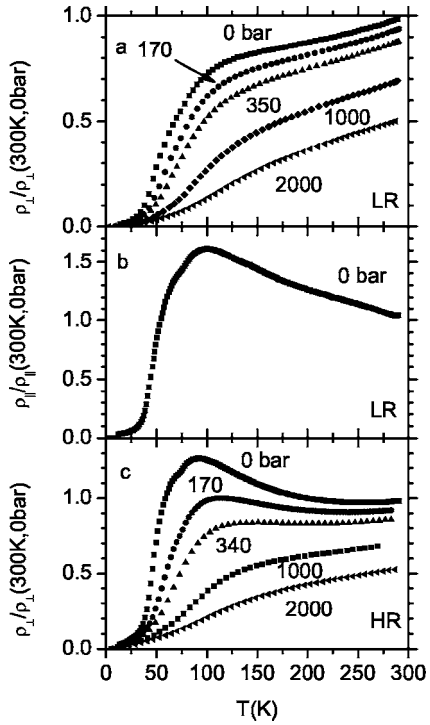

FIG. 2. Temperature dependence of the resistivity of single crystalline κ-(BEDT-TTF)$_2$Cu[N(CN)$_2$]Br at various hydrostatic pressure values up to 2000 bar. Measurements were performed on the low-resistance (LR) crystal with current perpendicular (a) and parallel (b) to the highly conducting planes and for a standard high-resistance (HR) sample perpendicular to the planes (c).

most strongly pronounced at intermediate temperatures 40 K$\lesssim T\lesssim$200 K, with a relative reduction $\rho^{-1}\Delta\rho/\Delta p = \rho(T,p_0=0)^{-1}[\rho(T,p_0)-\rho(T,p)]/(p_0-p)$ for $p=170$ bar corresponding to about $-(360\pm20)\%$ kbar^{-1} at 50 K and $-(180\pm15)\%$ kbar^{-1} at 80 K for the HR crystal. A somewhat smaller, though still very large, pressure response of $-(250\pm20)\%$ kbar^{-1} (50 K) and $-(120\pm10)\%$ kbar^{-1} (80 K) is found for the LR crystal. At higher temperatures, i.e., $T=200$ K and 250 K, the effect of pressure becomes substantially reduced reaching values of $-(45\pm5)\%$ kbar^{-1} and $-(35\pm5)\%$ kbar^{-1}, respectively, which is about the same for both crystals.

Figure 3 shows the low-temperature out-of-plane resistivity data for the LR and HR crystals on expanded scales. For the LR crystal [Fig. 3(a)], the midpoint (50% point) of the resistivity drop at ambient pressure is at (12.2 ± 0.07) K with a 10%–90% width of only 0.2 K. With increasing pressure, the transition shifts to lower temperatures and broadens progressively. Using the midpoint as a measure of T_c, we find an initial pressure coefficient of $dT_c/dp|_{p\to0}=-(2.6\pm0.2)$ K kbar^{-1}. These numbers have to be compared with $T_c=(12.0\pm0.07)$ K, a 10–90% width of 0.4 K and $dT_c/dp|_{p\to0}=-(2.4\pm0.2)$ K kbar^{-1} for the HR crystal [Fig. 3(b)]. The pressure coefficient of T_c for both crystals is in excellent agreement with the results of previous pressure studies yielding pressure coefficients of -2.4 K kbar^{-1} [6] and -2.8 K kbar^{-1} [7].

Common to the data sets for the LR and HR crystals in Fig. 2 is the almost abrupt change in $\rho(T)$ from a strongly

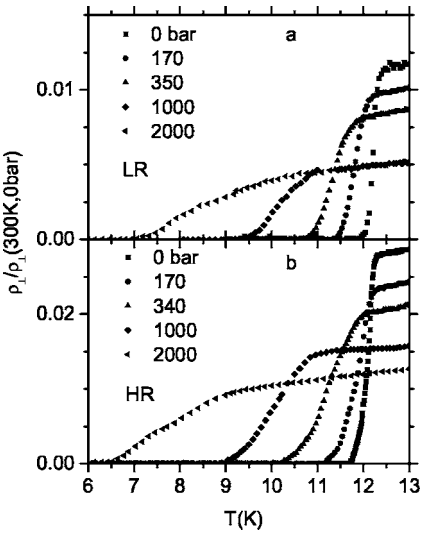

FIG. 3. Low-temperature out-of-plane resistivity data at various hydrostatic pressure values up to 2000 bar for the (a) low (LR)- and (b) high (HR)- resistance variant of κ-(BEDT-TTF)$_2$Cu[N(CN)$_2$]Br.

temperature-dependent behavior at intermediate temperatures to an only weakly temperature-dependent $\rho(T)$ at low temperatures.

This becomes even more clear in Fig. 4 where the derivative $d\rho_\perp/dT$ is plotted for the LR [Fig. 4(a)] and HR [Fig. 4(b)] crystals at different pressure values. For both samples, we find a pronounced maximum in $d\rho/dT$ at about the same temperature $T_{max}=44$ K in accordance with previous results on an HR crystal.[29] With increasing pressure, the maximum becomes reduced in size, rounded, and shifted to higher temperatures. At a pressure of $p=2$ kbar, the maximum has been

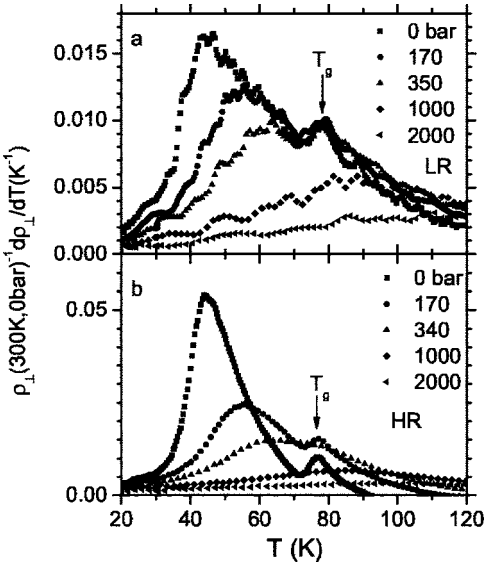

FIG. 4. Temperature derivative of the out-of-plane resistivity data for the (a) low (LR)- and (b) high (HR)- resistance variants of κ-(BEDT-TTF)$_2$Cu[N(CN)$_2$]Br at various pressures. Arrows indicate the glass-transition temperature at T_g associated with frozen-in disorder of the ethylene endgroups.

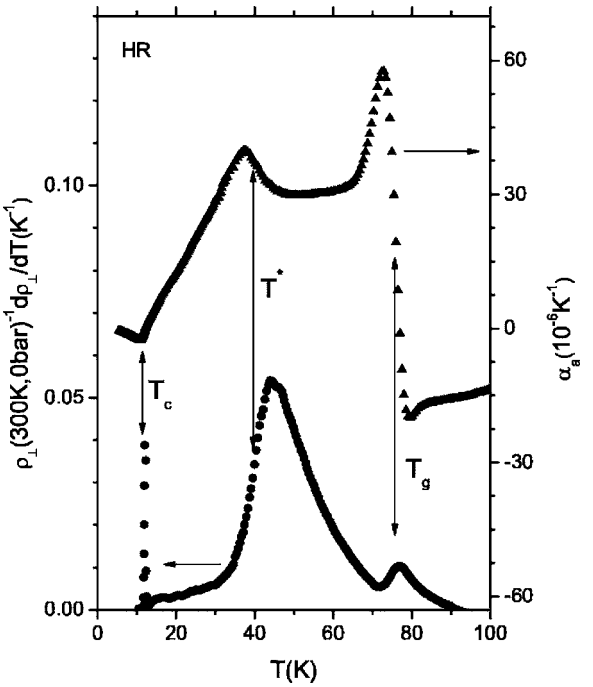

FIG. 5. Temperature derivative of out-of-plane resistivity data, $d\rho_\perp/dT$ (left scale) and thermal expansion results (right scale) taken from Ref. 28 for two different HR κ-(BEDT-TTF)$_2$Cu[N(CN)$_2$]Br crystals plotted on the same temperature scale. The resistivity data for $T \leqslant 10.5$ K have been omitted for clarity. Arrows indicate positions of the superconducting (T_c) and glass transition (T_g), as well as for the anomaly at T^*.

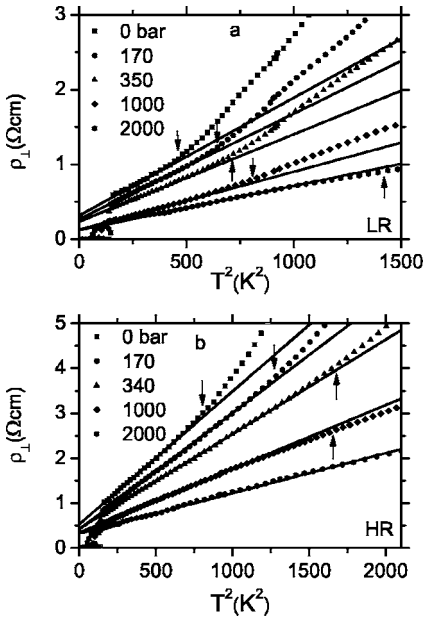

FIG. 6. Low-temperature out-of-plane resistivity data for the (a) low (LR)- and (b) high (HR)- resistance variant of κ-(BEDT-TTF)$_2$Cu[N(CN)$_2$]Br under various pressures plotted as a function of T^2. Arrows mark the temperatures where the data deviate by more than 2% from the straight lines.

suppressed almost completely. The sharp peak at the high-temperature side of the $d\rho/dT$ maximum in Fig. 4 reflects the glass transition. Its position is almost identical for both crystals with $T_g = 77$ K. With increasing pressure, the signature of the glass transition becomes weaker while its position remains almost unaffected up to $p = 170$ bar and, for the LR crystal, even up to $p = 350$ bar. The data yield an upper limit for the pressure coefficient of T_g of $dT_g/dp|_{p\to 0} \geqslant -0.6$ K kbar^{-1}. At higher pressures $p \geqslant 1$ kbar, however, an indication of the glass transition can no longer be resolved.

In Fig. 5 we compare the temperature dependence of the $d\rho_\perp/dT$ data of Fig. 4(b) with those of the coefficient of thermal expansion measured along the in-plane a axis, α_a, on a similar HR crystal.[28] According to Ref. 28, anomalous and strongly anisotropic behavior characterizes the uniaxial-expansion coefficients around 40 K with the largest effect in α_a. Since the latter governs the volume-expansion coefficient β in this temperature range and, moreover, reveals a well-pronounced signature also at the glass-transition temperature $T_g = 77$ K, where the response in β is rather small, the α_a data have been taken for the comparison in Fig. 5. The figure discloses a clear correspondence of the features in $d\rho/dT$ with the phase-transition-like anomalies observed in $\alpha_a(T)$ at $T_c = 12$ K, $T_g = 77$ K, and $T^* \simeq 40$ K.[28] More precisely, as indicated by the arrow at T^*, it is the midpoint of the low-T side of the $d\rho/dT$ maximum which coincides with the transition temperature T^* determined from $\alpha(T)$.[30] Using the midpoint as a measure of T^*, the data in Fig. 4 can be used to determine the pressure dependence of T^*. For pressures $p \leqslant 350$ bar, this criterion yields about the same pressure coefficient of $dT^*/dp|_{p\to 0} = +(35 \pm 7)$ K kbar^{-1} for both variants. This value slightly exceeds the pressure effect of about +25 K kbar^{-1} reported by Frikach *et al.*[31] who followed the position of the pronounced minimum in the sound velocity as a function of pressure.

Figure 6 shows the low-temperature interlayer resistivity data in a $\rho(T)$ vs. T^2 representation. In accordance with published results,[27,29,32] the normal-state resistivity of the HR crystal [Fig. 6(b)] follows a $\rho(T) = \rho_0 + AT^2$ behavior over an extended temperature range. From Fig. 6(b), we derive a coefficient $A^{HR} = (3 \pm 0.6)$ mΩ cm K^{-2} and a residual resistivity $\rho_0^{HR} = (530 \pm 100)$ mΩ cm. The error bars account for uncertainties implied in determining the geometric factor. A T^2 dependence is also found for the LR crystal [Fig. 6(a)] although with markedly smaller values for the coefficient A and the residual resistivity of $A^{LR} = (1.6 \pm 0.4)$ mΩ cm K^{-1} and $\rho_0^{LR} = (320 \pm 80)$ mΩ cm, respectively. In addition, Fig. 6 discloses significantly different validity ranges for the T^2 law for both variants. Using a 2% deviation of the straight lines in Fig. 6 as a measure for the upper boundary T_0 of the T^2 dependence, we find ambient-pressure values of $T_0^{LR} = (23 \pm 0.5)$ K and $T_0^{HR} = (28 \pm 0.5$K) for the LR and HR crystals, respectively. As indicated by the arrows in Fig. 6, both variants reveal a strongly nonlinear, and, for the HR crystal, even a nonmonotonous, change of T_0 with pressure, see Fig. 7(b). We note that the analysis of the in-plane data at ambient pressure of the LR crystal in Fig. 2(b) reveals a T_0^{LR} value which is identical to that derived from the out-of-plane resistivity.

Figure 7(a) compiles the relative changes of the coefficient A, $\Delta A/A(p=0) = A(0)^{-1}[A(p) - A(0)]$ (left scale) and the

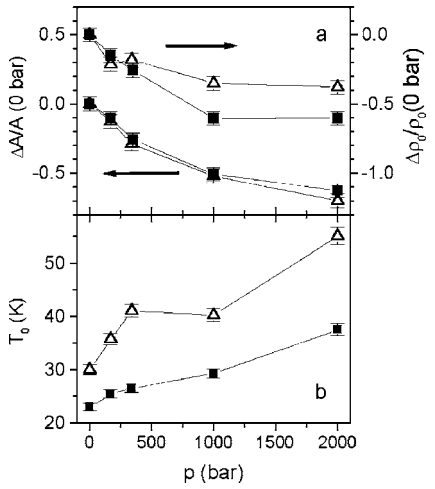

FIG. 7. (a) Relative change of the coefficient A, $\Delta A = A(p) - A(0\ \text{bar})$, and the residual resistivity ρ_0, $\Delta\rho_0 = \rho_0(p) - \rho_0(0\ \text{bar})$, and (b) absolute shift of the temperature T_0 as read off Fig. 6, with pressure for the low (LR) (filled squares)- and high-resistance (HR) (open triangles) variant of single crystalline κ-(BEDT-TTF)$_2$Cu[N(CN)$_2$]Br.

residual resistivity ρ_0, $\Delta\rho_0/\rho_0 = \rho_0^{-1}[\rho_0(p) - \rho_0(0)]$ (right scale) as a function of pressure. For the coefficient A, we find almost identical behavior for both crystals with a stronger reduction at small pressures and a weak pressure dependence at $p \geqslant 1$ kbar. A similar tendency can be inferred also for the residual resistivity, although here the pressure effect for the HR crystal is somewhat smaller and there is no significant pressure dependence for $p \geqslant 1$ kbar.

IV. DISCUSSION

As described in the experimental section, the LR and HR variants of κ-(ET)$_2$Cu[N(CN)$_2$]Br are the results of somewhat different preparation routes. The preparation conditions used for the crystals #2, #3, and the LR crystal essentially differ from the standard procedure in using a mixture of THF and EG as a solvent rather than TCE, although interrelations with the other preparation parameters cannot be ruled out completely. These differences may cause variations in the purity of the materials, i.e., the concentration and the nature of incorporations,[33] and the structural perfection. The latter refers to the degree and character of structural disorder.

According to the high-resolution x-ray diffraction studies performed here, there are no significant differences in the overall structural properties between crystals from both preparation routes. A possible Cl contamination was checked in the structure refinement by allowing for a partial occupation of the Br site by Cl with the result of 100% Br occupation consistent with our EPMA results. Further, no incorporation of solvent molecules was found in the crystal structure. Yet, minor amounts of solvent molecules distributed as point defects in the crystals cannot be excluded. A structural feature of particular relevance for the present material is the disorder of one of the ethylene end groups of the BEDT-TTF molecule associated with two different conformations of the molecule, the eclipsed form (both ethylene end groups are parallel) and the staggered form (ethylene end groups are nearly perpendicular to each other). At room temperature, the occupation factor of the eclipsed form refines to the same value of $(69 \pm 2)\%$ for both crystals. At 100 K the disorder is already considerably reduced as indicated by an occupation factor of $(92 \pm 2)\%$ of the eclipsed form—again identical within the experimental accuracy for both crystals.

The above results make clear that the identification of the preparation-dependent differences between the various crystals, i.e., the kind and degree of disorder and other real-structure phenomena, requires highest-resolution structural studies using synchrotron radiation. Since this information is not available yet, a general characterization of the crystals studied here is feasible on the basis of the present transport measurements.[34,35]

According to the residual resistivity ratio, which is the highest for the LR crystal (RRR=158) and the lowest for the HR one (67), the LR crystal is of distinctly superior quality. The HR crystal studied here, however, appears to be representative for most of the κ-(ET)$_2$Cu[N(CN)$_2$]Br crystals studied so far which had been prepared according to the standard procedure. These crystals yield room-temperature resistivities $\rho_\perp(300\ \text{K})$ and RRR values of 50–70 Ω cm and 50–65, respectively.[27,29,36] Moreover, the samples studied here reveal a clear correlation between the residual resistivity ratio and the size of the resistivity around 90 K: with increasing RRR from 67 over 84 and 89 to 158, the resistivity maximum around 90 K continuously decreases. We note that for the crystal studied in Ref. 37 yielding RRR=193 and a Dingle temperature of $T_D = (2 \pm 0.2)$K, $\rho_\perp(T)$ is almost identical to that found for the present LR crystal. According to the work by Stalcup *et al.*,[38] who studied temporal processes on the amplitude of Shubnikov–de Haas oscillations, a value of $T_D = 2$ K corresponds to the limit of a "most ordered" material.

The possibility of internal strain, which might account for the suppression of the anomalous resistivity maximum at intermediate temperatures for the LR crystal, can be safely discarded due to both the high T_c value and the very narrow 10%–90% transition width of only 0.2 K. The latter is a factor of 2 smaller than that which is usually encountered for this salt[27,29] and which is found also for the present HR crystal. At the same time, both variants behave almost identically with regard to the glass transition temperature $T_g = 77$ K, although the signature at T_g in the interlayer resistivity, i.e., the additional scattering contribution to $\rho_\perp$ for $T < T_g$, is stronger for the HR crystal. This might indicate a somewhat reduced fraction of frozen-in disordered ethylene groups in the LR compared to the HR sample.

It is fair to say that the influence of the glass transition on the low-temperature electronic properties in this class of materials has not been fully understood yet. While cooling-rate-dependent changes in the resistivity indicate changes in the scattering rate,[38] those in the ESR linewidth and spin susceptibility have been attributed to disorder-induced changes in the band structure.[23] We note that the difference in the resistivity profiles of the various crystals discussed here manifest themselves already at room temperature (cf. Fig. 1), i.e., way

above the glass transition temperature. Moreover, the very slow cooling and warming rates of ± 0.1 K min^{-1} employed in the present resistivity measurements, which result in cooling and warming curves that differ by less than 1% over the whole T range investigated, reduce the influence of the cooling-rate-dependent effects associated with the glass transition as much as possible. According to Ref. 38, where it has been demonstrated that the equilibrium curve, which corresponds to the most ordered ground state, lies between the nonequilibrium cooling and warming curves, the small hysteresis observed here indicates that the resistivity profiles are very close to these equilibrium curves. For the above reason and the fact that ESR and x-ray measurements lack any significant differences between samples from both preparation routes, we believe that the different resistivity profiles are not affected by cooling-rate dependent changes of the Fermi surface.

The most obvious difference between the HR and LR crystals highlighted in Fig. 1 is the distinct reduction of the $\rho(T)$ maximum at intermediate temperatures. Yet a remnant of this feature, though much less strongly pronounced, is still present for the LR sample, where it gives rise to an unusual $\rho(T)$ anisotropy with a metallic-type resistivity in the out-of-plane component but a semiconducting-like behavior for the in-plane resistivity.[39] We note, however, that the resistivity anisotropy $\rho_\perp/\rho_\parallel$ of about 100 at room temperature, derived from the present experiments (cf. Fig. 2) on an irregularly shaped crystal as compared to an anisotropy ratio in excess of 1000 reported by Buravov *et al.*,[29] determined on a plate-like HR crystal, indicates that the present $\rho_\parallel$ data still contain a significant interlayer component $\rho_\perp$.

A strongly reduced, though finite, scattering contribution around 90 K in the LR crystal is in line with the observation of a significant reduction of the still extraordinarily strong pressure response of the resistivity at intermediate temperatures compared to that of the HR crystal.

The above observation that the anomalous scattering contribution centered around 90 K differs strongly depending on the preparation conditions and becoming reduced in size upon increasing the sample quality, indicates that a significant part of the anomaly is extrinsic in nature. At this point, it is natural to ask whether the resistivity anomalies of related compounds are also subject to such preparation-dependent changes. Here we mention the strongly different resistivity profiles reported for the related κ-$(ET)_2Cu(NCS)_2$ compound, see, e.g., the papers by Ugawa *et al.*[40] and Urayama *et al.*[41] Interestingly enough, the crystal discussed in Ref. 40, where the resistance maximum is substantially reduced, had been prepared also by using THF as a solvent. These findings, which confirm the conclusions drawn here for the κ-$(ET)_2Cu[N(CN)_2]Br$ salt and underline the particular role of the solvent in the preparation process, demonstrate that disorder or defects may induce drastic changes in the temperature-dependent part of the resistivity, i.e., the inelastic scattering contributions. Such a behavior is highly unusual and at variance with what is known from ordinary metals, where the scattering due to disorder or impurities manifests itself in an increase of the residual resistivity only. This raises the fundamental question on how and to what extent disorder-or defect-induced potentials may affect the inelastic scattering of π electrons in the present molecular conductors.

Apart from these differences related to the anomalous resistivity contribution around 90 K, both variants behave identically as to the drastic change in their resistivity at $T = T^* \simeq 40$ K from a range characterized by a strongly T-dependent $\rho(T)$ at $T > T^*$ into a low-temperature regime, where $\rho(T)$ varies only weakly with temperature. It was found that the anomaly in $d\rho/dT$ coincides with the phase-transition-like feature observed in the coefficient of thermal expansion $\alpha(T)$. Such a direct correspondence of anomalies in transport and thermodynamic quantities is not expected for a crossover behavior between two different regimes, which usually involves a scaling factor to map the characteristic temperatures T_ρ and T_α. As an example, we mention the Kondo effect in heavy-fermion compounds, where the positions of rather broad signatures in $\rho(T)$ and $\alpha(T)$ differ by about 25% (see, e.g., Ref. 42). Rather the coincidence of distinct anomalies in $d\rho/dT$ and $\alpha(T)$ indicates that this feature marks a cooperative phenomenon.

Anomalous behavior around T^* has been also identified in various thermal,[7,28,29,43,44] magnetic,[21,45–47] elastic,[31] and optical properties.[48] Various explanations have been proposed as to the nature of the T^* anomaly, including the formation of a pseudo-gap in the density of states,[21,45,46,49] a crossover from a coherent Fermi liquid at low temperatures into a regime with incoherent excitations at high temperatures,[4,13] a density-wave-type instability,[28,44,50] as well as an incipient divergence of the electronic compressibility caused by the proximity to a Mott transition.[5] The present resistivity results, which for the HR crystal confirm published data,[29] clearly demonstrate that the position of the T^* anomaly is unaffected by the strength of the additional scattering contribution giving rise to the resistivity hump at intermediate temperatures, and thus marks an independent feature. In addition, the sharpness of the anomaly in $d\rho/dT$ and its direct mapping with the jump in the coefficient of thermal expansion makes it very unlikely that T^* merely reflects a crossover between two different transport regimes[51]—an assumption which underlies some of the above theoretical models. Rather it indicates that T^* reflects a phase transition into a symmetry broken low-temperature state.

Turning now to the $\rho = \rho_0 + AT^2$ behavior for $T \leqslant T_0 < T^*$, our study reveals a relative change with pressure of the coefficient A which is quite similar for the LR and HR crystals. This indicates that it is the same scattering mechanism which governs the low-temperature $\rho(T)$ behavior for both systems. However, the size of A is substantially reduced for the LR crystal reflecting a weakening of this scattering contribution for the higher-quality LR crystal.

There has been a long-standing debate on the nature of the T^2 behavior in the resistivity of molecular conductors. In fact, a $\rho \propto T^2$ dependence over an extended temperature range is not a peculiarity of the κ-phase $(ET)_2X$ salts alone. It has been observed also for various other materials such as the $(TMTSF)_2PF_6$ and the β-$(ET)_2X$ salts, see, e.g., Refs. 53–55.

The explanations proposed for the T^2 behavior in these materials include electron-phonon[56] as well as electron-

electron interactions of the strongly correlated π-electron system.[4,13,53] In fact, such a T^2 dependence at low temperatures is characteristic of metals in which the dominant scattering mechanism is provided by the electron-electron interactions. Since there the coefficient $A \propto (m^*)^2 \propto (T_F^*)^{-2}$, with m^* the effective carrier mass and T_F^* the effective Fermi temperature, the coefficient A scales with the square of the Sommerfeld coefficient $\gamma \propto m^* \propto (T_F^*)^{-1}$ of the electronic specific heat $C_{el} = \gamma T$. Such an $A/\gamma^2 = \text{const}$ behavior within a given material class has been verified for different systems including heavy-fermion compounds and transition metals,[57,58] (see also Ref. 59 for the quasi-2D system Sr_2RuO_4).

The above scaling implies that upon variation of a control parameter x of the system, such as chemical composition or external pressure, the product $A(x)\,[T_F^*(x)]^2$ should stay constant. By identifying the temperature T_0, i.e., the upper limit of the T^2 range in the resistivity, with the effective Fermi energy T_F^*, Limelette *et al.* have verified this invariance for pressurized κ-$(ET)_2Cu[N(CN)_2]Cl$.[4]

The results of the present studies, however, render such an interpretation unlikely. Given that the T^2 dependence is of electronic origin, i.e., $A \propto (T_F^*)^{-2}$ and $T_0 \simeq T_F^*$, the A coefficient for the LR variant, which is reduced by a factor of about 1.9 compared to that of the HR crystal, would then indicate an effective Fermi temperature T_F^* which is larger by a factor of $(1.9)^{1/2} \approx 1.4$. This is in contrast to the experimental observation yielding a T_0^{LR} which is even reduced by a factor of about 1.3 compared to that for the HR crystal. Rather, our experimental finding that both T_0 and A are strongly sample dependent while the other characteristic temperatures associated with the electronic properties such as T^* and T_c are not, indicate that the nature of the T^2 dependence is different from coherent Fermi-liquid excitations.[60,61] reveal that a significant part of the scattering contribution which gives rise to the anomalous resistivity maximum around 90 K in standard high-resistance materials is extrinsic in nature. Apart from this sample-dependent scattering contribution, however, both variants behave identically as to the abrupt change in $\rho(T)$ at $T^* \simeq 40$ K. The coincidence of this temperature with the phase-transition anomaly in the coefficient of thermal expansion makes it unlikely that T^* marks a crossover between two different transport regimes but rather indicates a second-order phase transition. For temperatures $T \leqslant T_0 < T^*$ the data for both crystals were found to follow a $\rho(T) \propto AT^2$. Most importantly, however, our analysis reveals strikingly different coefficients A and ranges of validity measured by T_0 for both variants. In view of the fact that other characteristic temperatures associated with the π-electron system such as T_c and T^* are sample independent, this strong variation in A and T_0 indicates an origin for the T^2 dependence different from coherent Fermi liquid excitations. The present results demonstrate that for these molecular materials, sample-dependent, i.e., extrinsic, factors such as disorder or defect concentration do not only change the elastic scattering contribution measured by the residual resistivity. Rather, the defect potentials may also strongly affect the temperature-dependent part of the resistivity, i.e., the inelastic scattering, indicating that Matthiessen's rule is no longer applicable to these materials. Consequently, the charge transport for available sample materials might be considerably affected by such extrinsic contributions. Detailed structural investigations on high- and low-resistance material are in progress in the hope of identifying the nature of the above scattering centers. This will help to control better the synthesis conditions and to provide eventually materials of sufficiently high quality which make it possible to access the intrinsic transport properties of these materials.

V. SUMMARY

Resistivity measurements under hydrostatic pressure on a low-resistance variant of the organic superconductor κ-$(BEDT\text{-}TTF)_2Cu[N(CN)_2]Br$ have been performed and compared to the results on a standard high-resistance crystal. The lower residual resistivity ρ_0 and the higher residual resistivity ratio $\rho(300\text{ K})/\rho_0$ for the low-resistance crystal clearly indicate its superior quality. These measurements re-

ACKNOWLEDGMENTS

The authors thank M. Kartsovnik and N. Toyota for fruitful discussions and suggestions. The work was supported by the Deutsche Forschungsgemeinschaft under the auspices of the Forschergruppe 412. Work at Argonne National Laboratory is supported by the Office of Basic Energy Science, Division of Material Science, U.S. Department of Energy, under contract No. W-31-109-ENG-38.

*present address: Forschungszentrum Rossendorf, Hochfeld-Magnetlabor Dresden (HLD), D-01314 Dresden, Germany

[1] K. Kanoda, Hyperfine Interact. **104**, 235 (1997).
[2] S. Lefebvre, P. Wzietek, S. Brown, C. Bourbonnais, D. Jérome, C. Mézière, M. Fourmigué, and P. Batail, Phys. Rev. Lett. **85**, 5420 (2000).
[3] H. Ito, T. Ishiguro, M. Kubota, and G. Saito, J. Phys. Soc. Jpn. **9**, 2987 (1996).
[4] P. Limelette, P. Wzietek, S. Florens, A. Georges, T. A. Costi, C. Pasquier, D. Jérome, C. Mézière, and P. Batail, Phys. Rev. Lett. **91**, 016401 (2003).
[5] D. Fournier, M. Poirier, M. Castonguay, and K. Truong, Phys. Rev. Lett. **90**, 127002 (2003).
[6] J. E. Schirber, D. L. Overmyer, K. D. Carlson, J. M. Williams, A. M. Kini, H. H. Wang, H. A. Charlier, B. J. Love, D. M. Watkins, and G. A. Yaconi, Phys. Rev. B **44**, 4666 (1991).
[7] Yu. V. Sushko, V. A. Bondarenko, R. A. Petrosov, N. D. Kushch, and E. B. Yagubskii, J. Phys. I **1**, 1015 (1991).
[8] I. D. Parker, R. H. Friend, M. Kurmoo, P. Day, C. Lenoir, and P. Batail, J. Phys.: Condens. Matter **1**, 4479 (1989).
[9] M. Kund, H. Müller, W. Biberacher, and K. Andres, Physica C **191**, 274 (1993).

[10] M. A. Tanatar, T. Ishiguro, T. Kondo, and G. Saito, Phys. Rev. B **59**, 3841 (1999).
[11] N. L. Wang, B. P. Clayman, H. Mori, S. Tanaka, J. Phys.: Condens. Matter **12**, 2867 (2000).
[12] M. Lang and J. Müller, in *The Physics of Superconductors* Vol. II, edited by K. H. Bennemann and J. B. Ketterson (Springer-Verlag, Berlin, 2004).
[13] J. Merino and R. H. McKenzie, Phys. Rev. B **61**, 7996 (2000).
[14] L. K. Montgomery, R. M. Vestal, K. P. Starkey, B. W. Fravel, M. J. Samide, D. G. Peters, C. H. Mielke, and J. D. Thompson, Synth. Met. **103**, 1878 (1999).
[15] V. A. Bondarenko, R. A. Petrosov, M. A. Tanatar, V. S. Yefanov, V. M. Ogenko, N. D. Kushch, and E. B. Yagubskii, Synth. Met. **70**, 955 (1995).
[16] M. A. Tanatar, T. Ishiguro, S. Kagoshima, N. D. Kushch, and E. B. Yagubskii, Phys. Rev. B **65**, 064516 (2002).
[17] A. M. Kini, U. Geiser, H. H. Wang, K. D. Carlson, J. M. Williams, W. K. Kwok, K. D. Vandervoort, J. E. Thompson, D. L. Supka, D. Jung, and M.-H. Whangbo, Inorg. Chem. **29**, 2555 (1990).
[18] Yu. Sushko, K. Andres, N. D. Kushch, and E. B. Yagubskii, Solid State Commun. **87**, 589 (1993).
[19] N. D. Kushch, L. I. Buravov, A. G. Khomenko, E. B. Yagubskii, L. P. Rosenberg, and R. P. Shibaeva, Synth. Met. **53**, 155 (1993).
[20] G. M. Sheldrick, SHELX97, program for the solution and refinement of crystal structures, University of Göttingen, Göttingen, Germany, 1997.
[21] V. Kataev, G. Winkel, D. Khomskii, D. Wohlleben, W. Crump, K. F. Tebbe, and J. Hahn, Solid State Commun. **83**, 435 (1992).
[22] T. Nakamura, T. Nobutoki, T. Takahashi, G. Saito, H. Mori, and T. Mori, Jpn. J. Phys. **63**, 4110 (1994).
[23] M. A. Tanatar, T. Ishiguro, T. Kondo, and G. Saito, Phys. Rev. B **61**, 3278 (2000).
[24] L. I. Buravov, N. D. Kushch, V. N. Laukhin, A. G. Khomenko, E. B. Yagubskii, M. V. Kartsovnik, A. E. Kovalev, L. P. Rozenberg, R. P. Shibaeva, M. A. Tanatar, V. S. Yefanov, V. V. Dyakin, and V. A. Bondarendo, J. Phys. I **4**, 441 (1994).
[25] N. Harrison, M. M. Honold, M. V. Kartsovnik, J. Singleton, S. T. Hannahs, D. G. Rickel, and N. D. Kushch, Phys. Rev. B **55**, R16005 (1997).
[26] J. Singleton and Ch. Mielke, Contemp. Phys. **43**, 63 (2002).
[27] X. Su, F. Zuo, J. A. Schlueter, M. E. Kelly, and J. M. Williams, Phys. Rev. B **57**, R14056 (1998).
[28] J. Müller, M. Lang, F. Steglich, J. A. Schlueter, A. M. Kini, and T. Sasaki, Phys. Rev. B **65**, 144521 (2002).
[29] L. I. Buravov, N. D. Kushch, V. A. Merzhanov, M. V. Osherov, A. G. Khomenko, and E. B. Yagubskii, J. Phys. I **2**, 1257 (1992).
[30] Note that in Ref. 28 T^* have been defined as the position of the maximum in the volume-expansion, coefficient while here the anomaly is treated as broadened second-order phase transitions, i.e., the transition temperature being located on the high-temperature flank of the $\alpha(T)$ anomaly.
[31] K. Frikach, M. Poirier, M. Castonguay, and K. D. Truong, Phys. Rev. B **61**, R6491 (2000).
[32] M. Dressel, G. Grüner, J. E. Eldridge, and J. M. Williams, Synth. Met. **85**, 1503 (1997).
[33] In Ref. 14 the influence of magnetic Cu(II) incorporations on the anomalous resistivity profiles has been investigated but no clear correlation has been obtained so far.
[34] In Ref. 35 the low-temperature thermodynamic properties on a crystal prepared in the same way as the present LR crystal have been studied by specific heat measurements.
[35] H. Elsinger, J. Wosnitza, S. Wanka, J. Hagel, D. Schweitzer, and W. Strunz, Phys. Rev. Lett. **84**, 6098 (2000).
[36] X. Su, F. Zuo, J. A. Schlueter, and M. E. Kelly, Solid State Commun. **107**, 731 (1998).
[37] J. Wosnitza, Physica C **317-318**, 98 (1999).
[38] T. F. Stalcup, J. S. Brooks, and R. C. Haddon, Phys. Rev. B **60**, 9309 (1999).
[39] Note that the directional-dependent studies by Buravov (Ref. 29) on an HR crystal reveal the same anisotropy with a peak in the resistivity around 90 K being strongest pronounced in the in-plane ρ_a and ρ_c data.
[40] A. Ugawa, G. Ojima, K. Yakushi, and H. Kuroda, Phys. Rev. B **38**, 5122 (1988).
[41] H. Urayama, H. Yamochi, G. Saito, K. Nozawa, T. Sugano, M. Kinoshita, S. Sato, K. Oshima, A. Kawamoto, and J. Tanaka, Chem. Lett. **1988**, 55.
[42] F. Steglich, G. Sparn, R. Moog, S. Horn, A. Grauel, M. Lang, M. Nowak, A. Loidl, A. Krimmel, K. Knorr, A. P. Murani, and M. Tachiki, Physica B **163**, 19 (1990).
[43] K. Murata, M. Ishibashi, Y. Honda, N. A. Fortune, M. Tokumoto, N. Kinoshita, and H. Anzai, Solid State Commun. **76**, 377 (1990).
[44] T. Sasaki, N. Yoneyama, A. Matsuyama, and N. Kobayashi, Phys. Rev. B **65**, 060505(R) (2002).
[45] H. Mayaffre, P. Wzietek, C. Lenoir, D. Jérome, and P. Batail, Europhys. Lett. **28**, 205 (1994).
[46] A. Kawamoto, K. Miyagawa, Y. Nakazawa, and K. Kanoda, Phys. Rev. Lett. **74**, 3455 (1995).
[47] P. Wzietek, H. Mayaffre, D. Jérome, and S. Brazovskii, J. Phys. I **6**, 2011 (1996).
[48] T. Sasaki, I. Ito, N. Yoneyama, N. Kobayashi, N. Hanasaki, H. Tajima, T. Ito, and Y. Iwasa, Phys. Rev. B **69**, 064508 (2004).
[49] S. M. De Soto, C. P. Slichter, A. M. Kini, H. H. Wang, U. Geiser, and J. M. Williams, Phys. Rev. B **52**, 10364 (1995).
[50] M. Lang, J. Müller, F. Steglich, J. A. Schlueter, A. M. Kini, and T. Sasaki, Synth. Met. **133-134** 107 (2003).
[51] We note that coinciding signatures in $d\rho/dT$ (Ref. 43) and the coefficient of thermal expansion (Ref. 50), similar in size and width to those shown in Fig. 5, have been reported also for the related κ-$(ET)_2Cu(NCS)_2$ compound at somewhat higher temperatures. This observation is at variance with the notion that these features originate from an incipient divergence of the electronic compressibility, because a substantial broadening of the signatures is expected for this compound which is located further away from the Mott-transition line. See, e.g., Ref. 52, for the broadening and reduction of the features in the sound velocity with increasing distance from the transition point.
[52] S. R. Hassan, A. Georges, and H. R. Krishnamurthy, cond-mat/0405359.
[53] L. N. Bulaevskii, Adv. Phys. **37**, 443 (1988).
[54] M. Weger, K. Bender, T. Klutz, D. Schweitzer, F. Gross, C. P. Heidmann, Ch. Probst, and K. Andres, Synth. Met. **25**, 49 (1988).
[55] M. Weger, M. Tittelbach, E. Balthes, D. Schweitzer, and H. J. Keller, J. Phys.: Condens. Matter **5**, 8569 (1993).
[56] M. Weger, J. Low Temp. Phys. **95**, 131 (1994); M. Weger and D. Schweitzer, Synth. Met. **70**, 889 (1995).

[57] K. Kadowaki and S. B. Woods, Solid State Commun. **58**, 507 (1986).

[58] K. Miyake, T. Matsuura, and C. M. Varma, Solid State Commun. **71**, 1149 (1989).

[59] Y. Maeno, K. Yoshida, H. Hashimoto, S. Nishizaki, S. Ikeda, M. Nohara, T. Fujita, A. P. Mackenzie, N. Hussey, J. G. Bednorz, and F. Lichtenberg, J. Phys. Soc. Jpn. **66**, 1405 (1997).

[60] The same conclusion has been drawn from pressure studies on the related compound β''-$(ET)_2SF_5CH_2CF_2SO_3$ by Hagel *et al.* (Ref. 61).

[61] J. Hagel, J. Wosnitza, C. Pfleiderer, J. A. Schlueter, J. Mohtasham, and G. L. Gard, Phys. Rev. B **68**, 104504 (2003).